Micellar Morphological Changes Promoted by Cyclization of PS-*b*-PI Copolymer: DLS and AFM Experiments

E. Minatti,[†,‡] P. Viville,[§] R. Borsali,[*,†] M. Schappacher,[†] A. Deffieux,[†] and R. Lazzaroni[§]

Laboratoire de Chimie des Polymères Organiques, LCPO-CNRS, ENSCPB and Bordeaux-1 University, 16 Avenue Pey Berland 33607 Pessac Cedex, France, Departamento de Química da Universidade Federal de Santa Catarina, Florianópolis, SC, Brazil, and Service de Chimie des Matériaux Nouveaux, Centre de Recherche en Sciences des Matériaux Polymères (CRESMAP), 20, Place du Parc, 7000 Mons, Belgium

Received June 13, 2002

ABSTRACT: We study the effect of the cyclization of a linear poly(styrene-*b*-isoprene) PS−PI copolymer on the morphology of the micelles formed in heptane (a selective solvent for PI). The linear and the cyclic copolymers have exactly the same degree of polymerization, i.e. 290 for PS and 110 for PI, i.e., volume fraction $\Phi_{PS} = 0.78$. We use dynamic light scattering (DLS) and atomic force microscopy (AFM) techniques to characterize the micellar morphology made from copolymer molecules, focusing on the effect of cyclization. We also report the concentration effect on the micelle size and shape made from the linear and cyclic copolymers. Our results show that the micelles made from linear PS−PI adopt a "classical" spherical shape and keep the same morphology parameters over the range of investigated concentrations. In contrast, the micelles arising from cyclic copolymer chains adopt a giant wormlike shape. In this later case, both the size and the shape evolve when the concentration is increased, starting from small individual "sunflower-like" micelles, at low concentrations, to giant wormlike micelles at higher concentrations. Our results suggest also that these giant wormlike micelles made from cyclic copolymer chains result from the self-assembly of "sunflower-like" elementary micelles.

Introduction

It is well documented that linear diblock and triblock copolymers can form micelles when dissolved in selective solvents (a solvent where only one of the blocks is soluble). During the past few decades, a large number of publications have been dedicated to the study of the properties of micelles that have revealed a great interest in both applied science and basic research. Consequently, an increasing number of industrial applications have been continuously discovered for these systems.[1−8] Besides the important fundamental aspects, copolymer micelles have been used, for instance, as drug carriers in drug delivery systems,[9,10] stabilizers in organic reactions,[11] and also as nanotemplates in nanotechnologies.[7,8]

Depending on the chemical nature of the copolymer, the micelles can be either formed in water or in organic solvents. In water, the micelles are formed from hydrophilic−hydrophobic diblock copolymer chains, where the core is constituted by the hydrophobic block and the corona by the hydrophilic block. Most of the work dealing with these micelles show that the micellar size, and thereby the aggregation number, is independent of the polymer concentration, but may evolve as a function of the temperature or the block copolymer composition.[1,2] Micelles were mainly described as having a spherical shape with a clear partition between the core and corona compartments. However, it has been demonstrated in numerous studies that micelles made from block copolymer chains can also adopt many other different morphologies,[3] such as cylinders,[5] rodlike,[1] wormlike,[6] vesicles,[11,12] hollow spheres,[7] or even branched tubules.[9] In those systems, the morphology of the diblock copolymer micelles strongly depends on the sample preparation,[12] the temperature,[4] the volume fraction,[13] and the concentration.[4]

It is generally also recognized that amphiphilic block copolymers can form micelles in organic media. Micellar organizations, however, can also be obtained when blocks are both hydrophobic, but chemically different. This is due to the affinity of the two blocks toward a common organic solvent. The most common systems are constituted by aliphatic block attached to aromatic block. For instance, polystyrene−polyisoprene diblock copolymer is a good candidate to promote such micellar organizations and has been widely described in the literature. PS−PI copolymers can form micelles in selective solvents for the PI block (e.g., *n*-alkanes,[14] such as heptane, decane, or dodecane) or for the PS segment (e.g., small ketones, DMF,[14] DBP[5]). As reported in the literature, at relatively low concentrations of block copolymer chains, the formed PS−PI micelles are usually spherical shaped[2] and their size and morphology are independent of the concentration. The core is very compact, and because of the insolubility of the inner block, these micelles are frozen and do not exchange any unimers.[10] In some cases, however, such as PS−PI in decane, the micelles formed are mobile,[15] implying that the PS core is swollen.

From a synthesis point of view, the chain end functionalities that are present at the two extremities of a linear copolymer can be covalently bound in order to form a copolymer ring. Theoretical studies predict sensitive differences between the properties of the linear and the cyclic copolymer[16−21] in the disordered state.

* Corresponding author. E-mail: borsali@enscpb.fr.
† LCPO-CNRS, ENSCPB, and Bordeaux-1 University.
‡ Departamento de Química da Universidade Federal de Santa Catarina.
§ Centre de Recherche en Sciences des Matériaux Polymères (CRESMAP).

10.1021/ma020927e CCC: $25.00
Published on Web 04/29/2003

Scheme 1. Topological Constraints on the Micelle Formation in Cyclic Diblock Copolymers as Compared to Simple Linear Diblock or Triblock Copolymers[a]

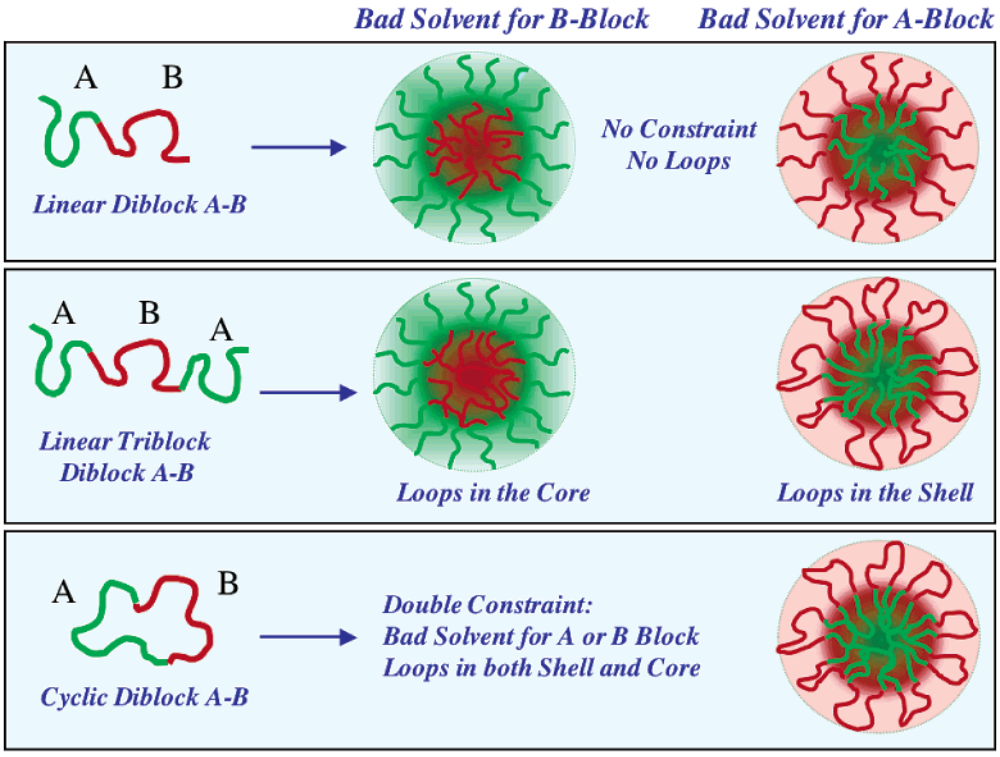

[a] A cyclic diblock AB copolymer combines both, a "looped" core and a "looped" shell, thus giving a "double constraint" effect on micelle formation.

Some of these properties were already highlighted using small-angle neutron scattering.[22] To our knowledge, there is no experimental data in the literature relating the properties of the micelles formed with the topology (cyclic vs linear) of PS−PI copolymer chains, except some preliminary results[23,24] that showed indeed sensitive differences in both micellar systems. The purpose of this work is to study the effect of the cyclization of PS−PI copolymer chains, as compared to linear diblock copolymers having exactly the same molecular weight and block composition, on their micellar organization. The average degree of polymerization (DP_n) of the two blocks is kept constant (290 for PS and 110 for PI). In this study, we have used dynamic light scattering (DLS) and atomic force microscopy (AFM) to characterize the evolution of the geometrical parameters (the size and shape) of the micelles both in solution (DLS) and in the solid-state (AFM), by evaporating the solvent. We have also investigated the effect of concentration on the morphology in both linear and cyclic copolymer systems.

At this stage, one should emphasize more on the importance and the motivations of this work. This study intended to answer the question of the topological constraints on the micelle formation in cyclic block copolymers as compared to simple linear diblock or triblock copolymers. In selective solvent for the B blocks, ABA triblock copolymer chains form sunflower micelles with A forming the core and B the outer loop. The same ABA triblock copolymer form micelles with B forming the core (i.e., the loop is in the core), such as in pluronics systems [25−37] in selective solvent for the B block. Our system, cyclic diblock AB copolymer, combines both a "looped" core and a "looped" shell, thus investigating the effect of a "double constraint" on micelle formation (see Scheme 1). We will show in this paper that this "double constraint" induces remarkable and sensitive changes in the morphologies of the micelles made from linear and from cyclic copolymer chains.

Scheme 2

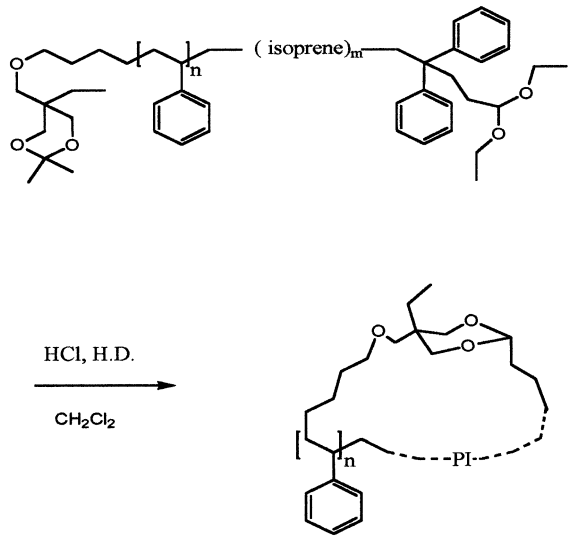

Experimental Section

The cyclic poly(styrene−isoprene) was prepared by direct coupling of α-isopropylidene-1,1-dihydroxymethyl-ω-diethylacetal-heterodifunctional linear poly(styrene-*b*-isoprene), previously prepared by living anionic polymerization (see Scheme 2). This method of synthesis permits to have exactly the same DP for each block PS and PI for linear and cyclic copolymer systems.[38]

As shown in Table 1, the average degree of polymerization of the poly(isoprene) block is roughly one-third of the DP for the poly(styrene) block for both the linear and cyclic copolymers. The linear and the cyclic copolymers have exactly the

Table 1. Characteristics of the Copolymers Used in This Work

copolymer	DP_{PS}	DP_{PI}	$M_w/10^3$ g/mol[a]
linear PS−PI	290	110	37
cyclic PS−PI	290	110	37

[a] The molar mass was determined by MALS-GPC analysis. The polydispersity index is less than 1.1 for both copolymer chains.

same degree of polymerization, i.e., 290 for PS and 110 for PI, i.e., volume fraction $\Phi_{PS} = 0.78$. At this molar weight and volume fraction, the micelles made from the PS−PI copolymer in a selective solvent for PI are expected to exhibit a large core (PS) and a short corona[13] (PI). In the case of linear PS−PI, these micelles should be spherical, and the present work is intended to discuss their morphology in the case of cyclic PS−PI diblock copolymers.

A. DLS Experiments. Sample Preparation. All the samples were prepared by adding the required amount of heptane (a bad solvent for PS) to the copolymer chains and then leaving them stirring for 72 h at 50 °C under inert atmosphere. Each sample was prepared individually; i.e., no dilution was made. All the solvents were HPLC grade and were distilled and filtered through a 0.2 μm PTFE membrane prior to use.

The light-scattering measurements were performed using an ALV laser goniometer, which consists of a 22 mW HeNe linear polarized laser with 632.8 nm wavelength and an ALV-5000/EPP multiple τ digital correlator with 125 ns initial sampling time. The samples were kept at an exact and constant temperature of 25.0 °C during all the experiments. The accessible scattering angle range is from 10 up to 150°. However, all the scattering measurements were done at 90°. The solutions were put in 10 mm diameter glass cells. The minimum sample volume required for the experiment was 1 mL. The data acquisition was done with the ALV Correlator Control software, and the counting time varied for each sample from 300 up to 600 s.

B. AFM Experiments. Samples (thin films) for AFM analysis were prepared by solvent casting at room temperature, starting from a solution in heptane (from 0.1 to 5 mg/mL). Typically, 20 μL of the solution was cast on a 1 × 1 cm^2 piece of freshly cleaved mica. Samples were analyzed after complete evaporation of heptane at room temperature.

The AFM microscope has been operated in tapping mode (TM), a procedure that is known to minimize the sample distortion due to mechanical interactions between the AFM tip and the surface. To further optimize the imaging, the ratio between the set point amplitude and the amplitude of the free-oscillating cantilever (A_{sp}/A_0) was adjusted to avoid an excessive loading force applied to the sample and possible squeezing of the material between the tip and the substrate. Under these conditions, TM−AFM can provide three-dimensional imaging of the surface morphology with very accurate lateral and vertical resolution without damaging the surface.[39,40] All TM−AFM images were recorded in ambient atmosphere at room temperature with a Nanoscope IIIa (Veeco, Santa Barbara, CA). The probes are commercially available silicon tips with a spring constant of 24−52 N/m, a resonance frequency lying in the 264−339 kHz range, and a typical radius of curvature in the 10−15 nm range. In this work, we present topography images that are recorded with the highest sampling resolution, i.e., 512 × 512 data points.

Results and Discussion

From the DLS experiments, the autocorrelation functions measured in both systems (micelles made from linear and cyclic PS−PI) at $\theta = 90°$ are shown in Figure 1, for two solutions at the same copolymer concentration (2 mg/mL) in heptane. The relaxation time for the cyclic PS−PI is higher than the one for the linear copolymer, reflecting a lower diffusion coefficient for the cyclic diblock. The values of the hydrodynamic radii were

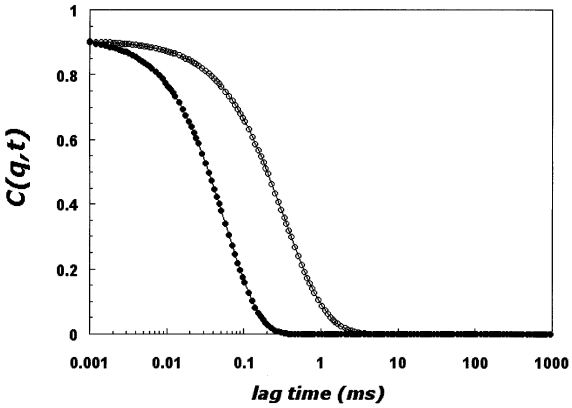

Figure 1. DLS autocorrelation functions on micelles formed from (●) linear PS−PI and (○) cyclic PS−PI at 2 mg/mL solutions in heptane.

calculated from the decay times using the Stokes−Einstein equation. The CONTIN analysis[41] of the DLS correlation functions for the linear and the cyclic PS−PI copolymer solutions are shown at different concentrations in Figures 2 and 3, respectively. In Figure 2 is illustrated CONTIN analysis from the DLS correlation functions of linear PS−PI copolymers at (A) 0.01, (B) 0.5, (C) 2.0, and (D) 5.0 mg/mL solutions in heptane. In Figure 3 is shown the CONTIN analysis from the DLS correlation functions of cyclic PS−PI copolymers at (A) 0.01, (B) 0.5, (C) 2.0, and (D) 5.0 mg/mL solutions in heptane. On one hand, for the linear PS−PI copolymer, CONTIN peaks always appear at the same hydrodynamic radius (R_H) value, meaning that the size of the linear PS−PI micelles does not change with the concentration. Moreover the peaks always exhibit the same narrow profile, which means that the formed micelles have a low polydispersity. On the other hand, the CONTIN profiles for the cyclic PS−PI micelles show that both the size and the polydispersity are concentration dependent.

From the Stokes−Einstein equation, the hydrodynamic radius (R_H) can be calculated from the DLS correlation function cumulant analysis.[42,43] Figure 4 shows the variation of the hydrodynamic diameter ($2R_H$) as a function of the concentration for the cyclic and the linear PS−PI micelles. The results show that the size of the linear PS−PI micelles remains constant for the whole investigated range of concentration (∼50 nm) whereas the size of the cyclic PS−PI micelles undergoes an important increase when the copolymer concentration is increased. For micelles made from linear copolymers, the reported R_H values as a function of the concentration correspond to the unique narrow relaxation mode that does not change with the concentration. As for the micelles made from cyclic copolymer chains, at very low concentration, R_H is the value deduced from the unique relaxation mode, and at higher concentrations we have taken an average of the multimodal distribution. This is justified since the AFM experiments have shown a polydisperse micellar morphologies (see Discussion below). Along the same line, this evolution of the size with the concentration has been also revealed when using static light-scattering experiments. Indeed, the apparent aggregation numbers N_{agg}^{app} for the micelles estimated at $c = 2$ mg/mL in heptane are $N_{agg}^{app} = 847$ for linear and $N_{agg}^{app} = 1001$ for cyclic ones. These values correspond to an apparent molecular weight of $M_w^{app} = 3.2 \times 10^7$ in the case of linear and $M_w^{app} = 3.8 \times$

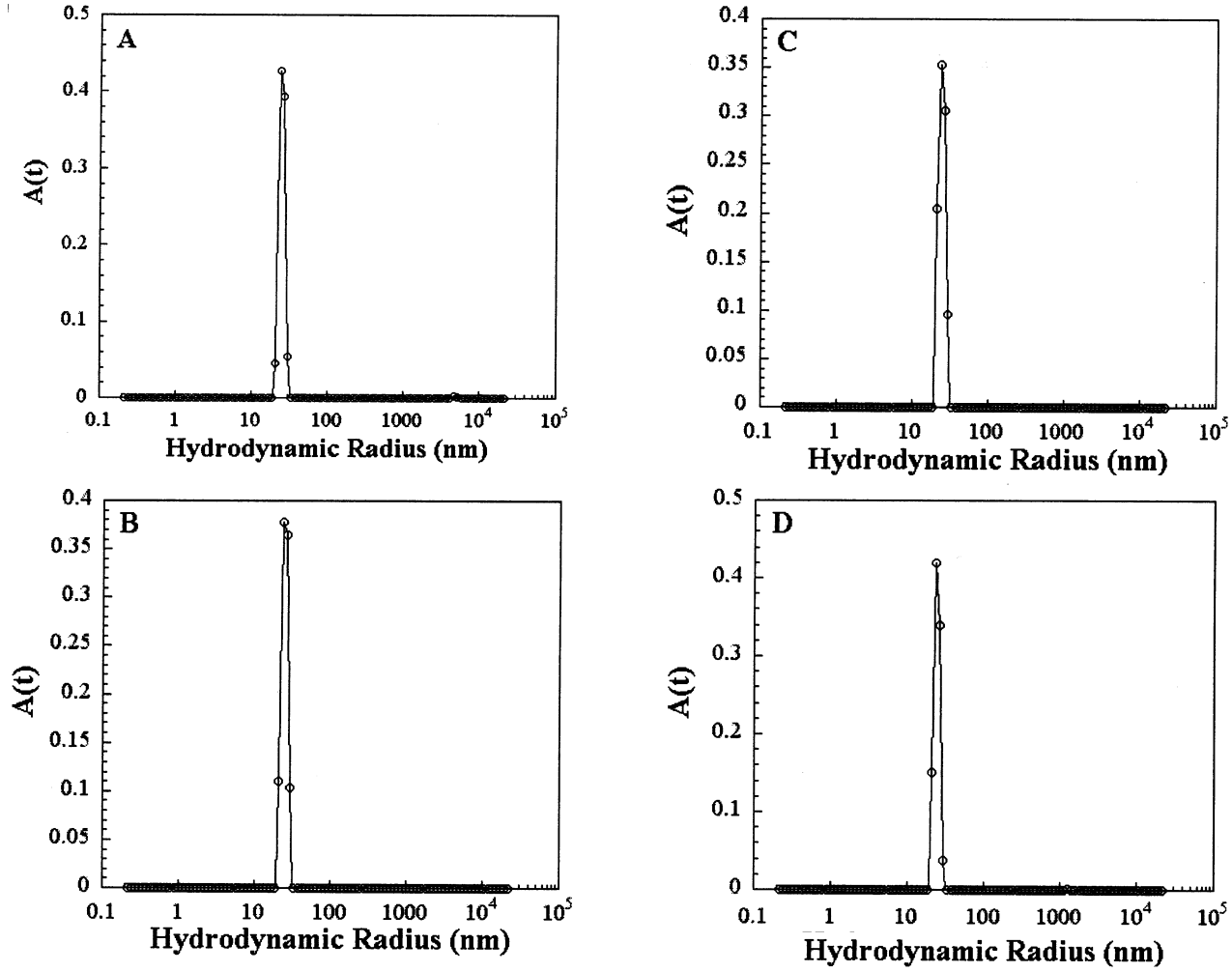

Figure 2. CONTIN analysis from the DLS correlation functions of linear PS−PI copolymers at (A) 0.01, (B) 0.5, (C) 2.0, and (D) 5.0 mg/mL solutions in heptane.

10^7 in the case of cyclic. While the aggregation number N_{agg}^{app} in spherical micelles made from linear copolymer is constant, that of micelles made from cyclic copolymer is an increasing function of the concentration. Both results obtained from static and dynamics scattering experiments clearly show that the size of the formed micelles is changing as a function of the copolymer concentration in the case of the cyclic PS−PI, whereas it is insensitive to the concentration in the case of micelles made from the linear diblock.

Another way to promote the growth of cyclic PS−PI micelles, other than increasing the copolymer concentration, is to decrease the solubility of the inner block toward the solvent. In our case, the solubility of PS increases with the number of carbons in the alkane chain used as a selective solvent, PS being more soluble in decane than in heptane. Indeed, we do not observe any substantial change in the size of the linear PS−PI micelles for a homologous alkane series. In contrast, the size of the cyclic PS−PI micelles should depend on the length of the alkane chain. This was indeed experimentally confirmed, as illustrated in Figure 5. The dimensions of the cyclic PS−PI micelles strongly increase with a decreasing number of carbons in the alkyl chain. The effect of decreasing the solvent quality for the inner block is thus comparable to the effect produced by increasing the copolymer concentration. For this reason, the dependence of the cyclic PS−PI micelle size with the copolymer concentration is less pronounced in decane than in heptane, as shown in Figure 6. One notes that the micelles made from linear PS−PI micelles have the same size in both solvents and does not show any dependence with the copolymer concentration.

It is well-known that for this range of molecular mass ($M_w = 37 \times 10^3$) and volume fraction $\Phi_{PS} = 0.78$, the micelles made from linear PS−PI are spherical[44] and that their size is mostly conditioned by the length of the inner block. Since the average degree of polymerization of the constitutive segments is the same for the linear and the cyclic systems, the rapid increase of the size for the cyclic copolymer micelles can only be explained in terms of a nonspherical morphology: longer objects (wormlike micelles) are formed when more copolymer chains are added to the solution. Under these conditions, the wormlike micelles would originate from the self-assembly of elementary "nonspherical" micelles termed hereafter "sunflowers". This is also supported by the polydispersity in size highlighted in the CONTIN analysis (see Figure 3) that shows the coexistence of objects having different lengths within the micelles made from cyclic PS−PI chains.

To have a more accurate description of the micellar morphology, we studied thin films of both the linear and the cyclic copolymers by direct imaging technique such as AFM. The first collection of AFM images corresponds to the morphology of the micelles made from linear

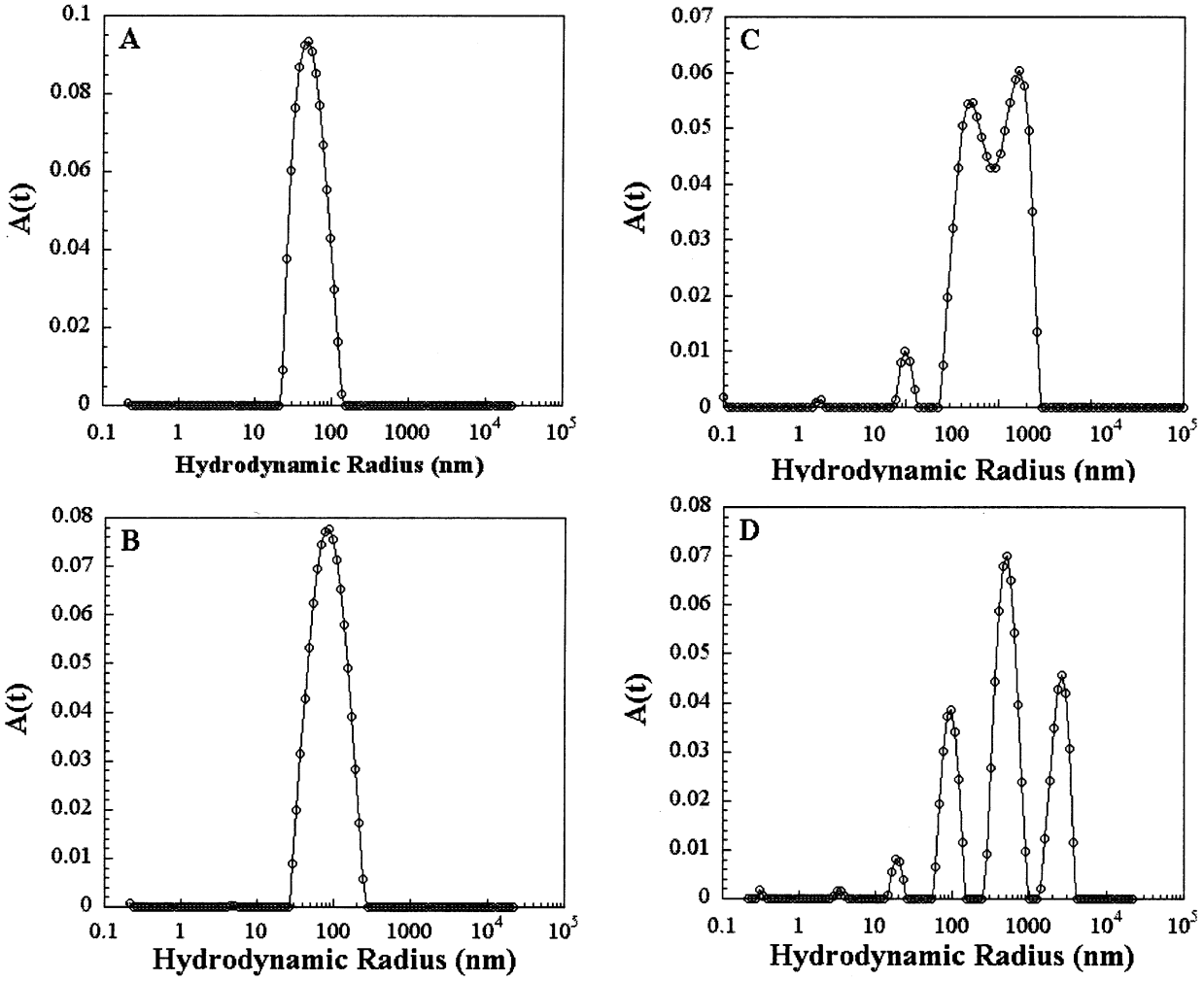

Figure 3. CONTIN analysis from the DLS correlation functions of cyclic PS−PI copolymers at (A) 0.01, (B) 0.5, (C) 2.0, and (D) 5.0 mg/mL solutions in heptane.

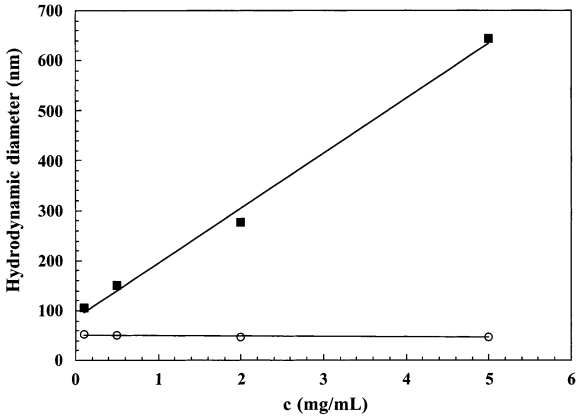

Figure 4. Hydrodynamic diameter ($2R_H$) for linear PS−PI (○) and cyclic PS−PI (■) copolymer solutions in heptane. The solid lines are guide for the eyes.

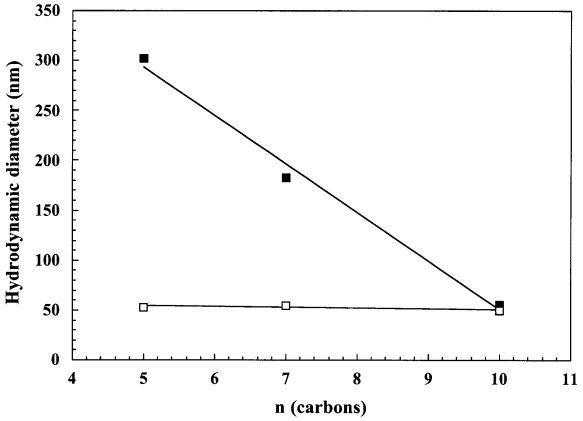

Figure 5. Hydrodynamic diameter from DLS measurements as a function of the number of carbon in *n*-alkane solvents (C_nH_{2n+2}), for the cyclic PS−PI copolymer (■) and the linear PS−PI copolymer (□). The concentration of all solutions is 1.0 mg/mL. The solid lines are guide for the eyes.

copolymer illustrated in Figure 7. As expected, we see that the micelles are spherical; they have a very narrow size dispersity and exhibit an average diameter equal to 40 ± 0.6 nm. One notes that this value is slightly smaller than the diameter $2R_H$ obtained from the DLS measurements (∼50 nm). This difference originates probably from the presence of the solvent in the case of the DLS experiments, inducing the swelling of the micelle corona. A cross-sectional analysis of the micelles is shown in inset D; it shows that the micelles are not perfect spheres. Modifying the ratio between the set point amplitude and the amplitude of the free oscillating cantilever (A_{sp}/A_0) does not modify the height of the micelles. An important observation is that the size and the shape of the micelles are independent of the concentration of the copolymer solution, as illustrated in Figure 7. Indeed, at low concentration (0.1 mg/mL, Figure 7A), individual spherical micelles or small as-

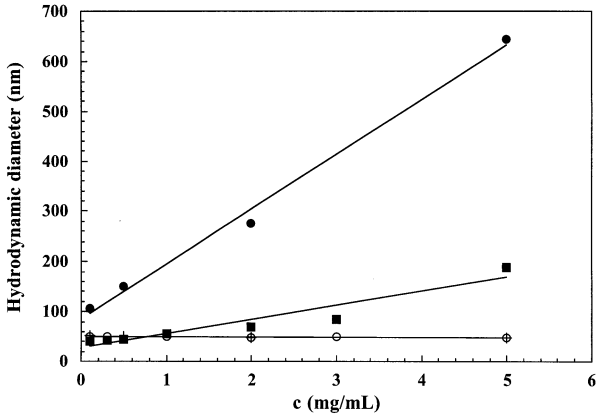

Figure 6. Hydrodynamic diameter from DLS measurements as a function of the copolymer concentration, for the cyclic PS−PI copolymer in decane (■), the cyclic PS−PI copolymer in heptane (●); the linear PS−PI copolymer in decane (+), and the linear PS−PI copolymer in heptane (○). The solid lines are guide for the eyes.

semblies of micelles are formed and are dispersed on the mica surface. Local analysis of their packing shows that the packing is mostly hexagonal. As the concentration of the solution is increased (from part A to part C), the micelles are found to be more and more densely packed, and in the extreme case, an homogeneous monolayer is formed, in which micelles can locally pack into different patterns (Figure 7C). As an illustration, areas marked #1 and #2 highlight two locations where the micelles adopt either hexagonal or cubic packing, respectively (Figure 7C).

It is important to note here that these observations are in good agreement with the DLS data, since the effect of adding more copolymer chains only promotes the formation of more micelles and increases their compactness. The size and the shape of these micelles remain constant over all the studied concentration range.

The results obtained for the cyclic copolymer micelles are interestingly different and illustrated in Figure 8.

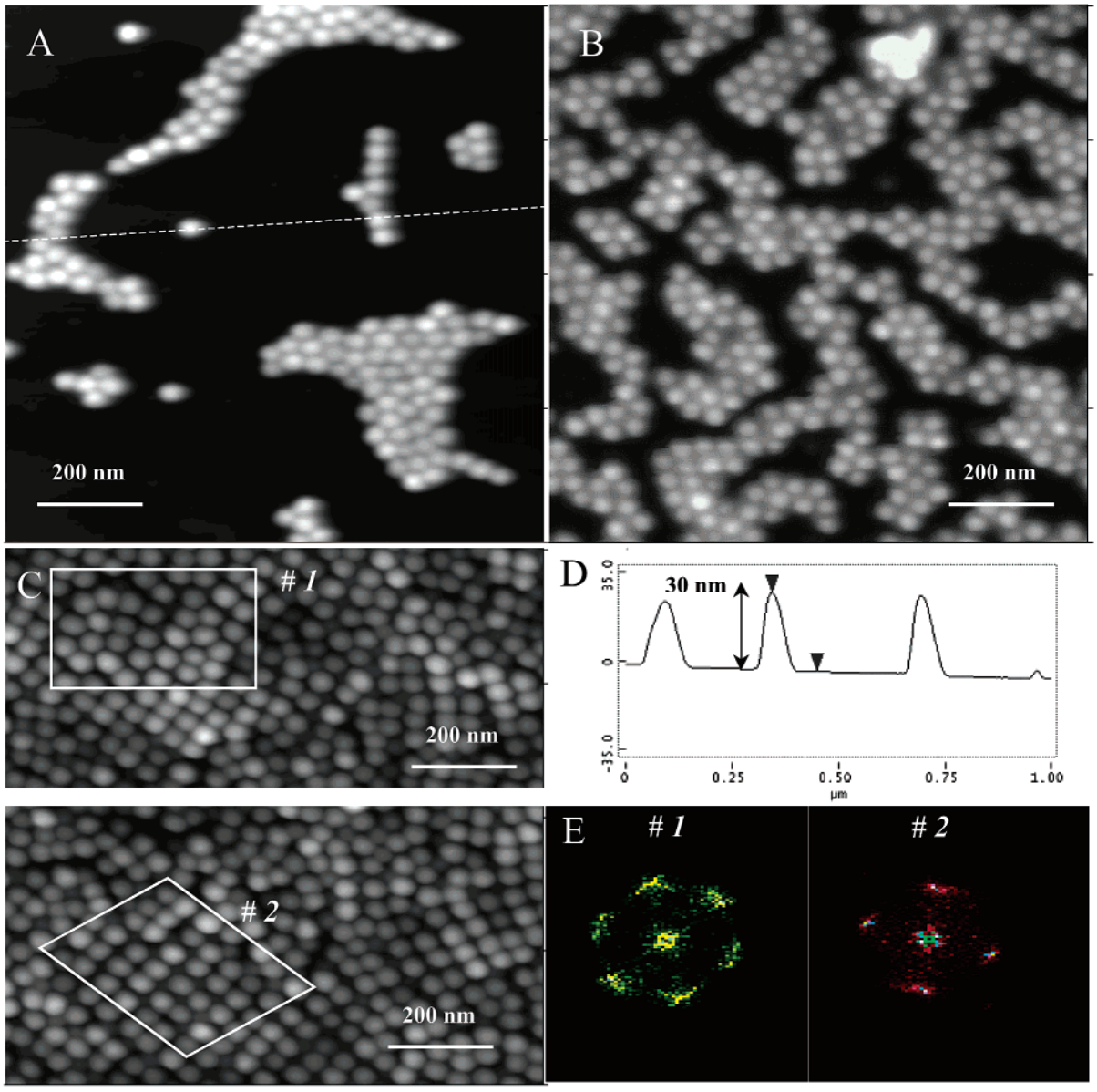

Figure 7. TMAFM topography images ($1 \times 1\ \mu m^2$) of linear PS−PI micelles obtained from solutions in heptane: (A) 0.1, (B) 1.0, and (C) 5 mg/mL. (D) Sectional analysis across the micelles. (E) 2D-Fourier transforms of the two selected areas in part C, illustrating the local hexogonal and cubic packing, respectively. The *Z* scale is 50 nm for all the images.

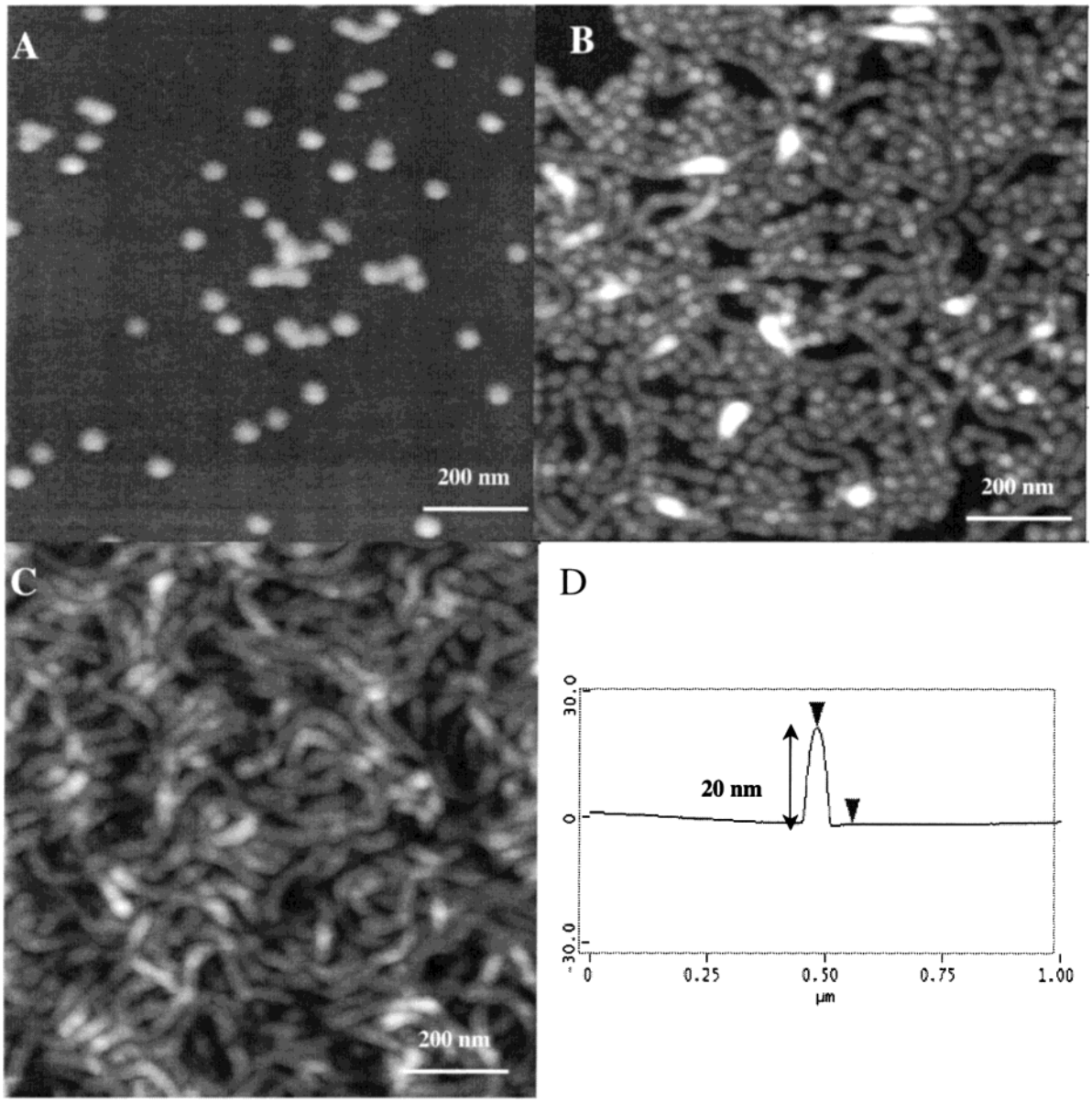

Figure 8. TMAFM topography ($1 \times 1\ \mu m^2$) images of cyclic PS−PI micelles obtained from solutions in heptane: (A) 0.1, (B) 1, and (C) 5 mg/mL. (D) Sectional analysis across the micelles. The *Z* scale is 50 nm for all the images.

At very low concentration (0.1 mg/mL), one observes isolated micelles that present a "spherical" shape (Figure 8A). Depending on the deposition conditions, these micelles can be found as isolated objects (Figure 8A) on the surface[45] or as small clusters (not shown here). The cluster formation is controlled by the rate of evaporation of the solvent during the sample preparation. Interestingly, the size of these micelles is smaller than that of the linear copolymer (33 nm vs 40 nm, respectively). Along the same line, the height of the micelles is smaller as compared to the one made from the linear copolymer (20 nm vs 30 nm); this is shown in the cross-sectional analysis (D) of Figure 8. With identical degrees of polymerization for the linear and the cyclic copolymer, this result confirms the existence of a different organization of the cyclic copolymer molecules within the micelles. One may here speculate that these elementary micelles have discoidal shape and are the so-called "sunflower". Another interesting observation is the disappearance of a regular organization in the clusters, which tends to demonstrate that the intermicellar assembly is also affected by the cyclization.

As the concentration is increased to an intermediate value ($c = 1$ mg/mL), a new morphology starts to develop. Indeed, both spherical micelles and longer objects (cylinders or *wormlike*) are found to coexist on the surface (Figure 8B). Since the diameter of these cylinders is equal to the diameter of individual micelles (33 nm), we may reasonably conclude that these particles are wormlike micelles formed by the self-assembly of individual elementary discoidal or "sunflower" micelles.

At high concentration (5.0 mg/mL), only wormlike micelles are found on the surface (Figure 8C). These micelles are entangled and their extremities are hardly discernible. Although the wormlike micelles seem to exhibit a wide range of lengths, their cross-section diameter is always equal to ~33 nm, i.e., smaller than the diameter of the micelles made from linear PS−PI copolymer.

One observes here that, contrary to micelles made from linear PS−PI copolymer, the size of the wormlike micelles measured by AFM cannot directly be compared to the size value obtained from DLS experiments, since

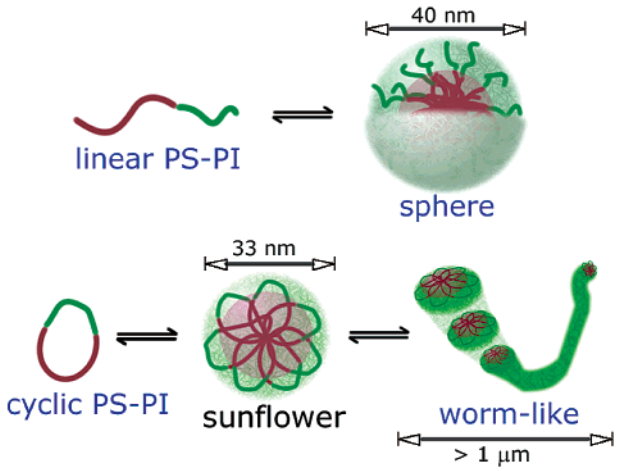

Figure 9. Sketch showing the core and corona of a wormlike micelle and the proposed morphology for the elementary *sunflower*-like micelle made of the cyclic PS−PI copolymer. The drawing also shows the structure of a spherical micelle made of the linear PS−PI copolymer.

the determination of R_H in principle applies to hypothetical spheres and not to anisotropic objects. Instead, the R_H value extracted from the correlation function cumulant analysis corresponds to average dimensions (equivalent sphere) of the cyclic PS−PI micelles.

In this work, DLS and AFM results were found to be in excellent agreement, demonstrating the strong evolution of the micellar organization as a function of both the cyclization of the copolymer molecules and the concentration of the copolymer solution. All the results converge to the same conclusion: asymmetric cyclic PS−PI copolymer molecules do not self-assemble under the form of "classical" spherical micelles. Instead, they organize within what we have called elementary "*sunflower-like*" micelles. They are promoted by the cyclization of the blocks, which introduces a loop in the copolymer chain (see Scheme 1 and Figure 9, top). As illustrated, the PI segments are forced to loop back to the core because of the cyclization and are, at the same time, exposed to the solvent in order to minimize the PS-solvent interface. Since the PI blocks are shorter than the PS segments (110 vs 290 corresponding to a volume fraction $\Phi_{PS} = 0.78$), the looping of the PI blocks in the micelle corona and the presence of a dense PS core form a "*sunflower-like*" micelle. Considering this morphology, it becomes clear that both the core and the corona length of the cyclic copolymer micelles are shortened compared to spherical micelles obtained from the corresponding linear PS−PI copolymer. The top of Figure 9 illustrates the two different types of morphologies for the micelles; on this basis, the observed differences between the micelle diameters can be understood. At very low concentrations, these sunflower-like micelles are present in solution as isolated objects. However, at relatively high concentrations, the cyclic copolymer molecules organize within an energetically more favorable wormlike morphology. As opposed to the spherical micelles formed from linear copolymers, the wormlike micelles result from the self-assembly in one direction of the "*sunflower-like*" elementary micelles whose architecture strongly favors the core−core attraction. In this self-assembled structure, the PS segments are still confined in a core unexposed to the solvent, allowing the microphase separation between the PS segments and the solvent (the driving force for the micelle formation) to occur. The bottom scheme in Figure 9 illustrates this morphology by showing a growing wormlike micelle and the *sunflower-like* micelle as the elementary unit.

The evolution from elementary *sunflower-like* to wormlike micelles as a function of the concentration is induced by a higher number of cohesive collisions between neighboring micelles. At high concentrations, all the sunflower micelles are stacked together to form giant wormlike micelles (see Figure 8C).

Along the same line, this wormlike morphology also supports the evolution of the size of the cyclic PS−PI micelles as a function of the solvent quality, which was highlighted by the DLS measurements (Figure 5). Indeed, let us recall that larger micelles of the cyclic copolymer are formed when the number of carbons in *n*-alkane solvents is decreased: e.g., from decane to pentane. This is explained by the fact that the thermodynamic stability of isolated sunflower-like micelles is reduced when the solubility of the PS segments toward the solvent is decreased, leading these objects to stack more readily into longer wormlike micelles. The stacking is allowed since the *sunflower-like* micelles present a more-opened (discoid) morphology compared to the spherical micelles of the linear system. According to the wormlike model, the ratio between the amount of wormlike and sunflower-like micelles is thus higher in heptane than in decane at intermediate concentrations ($c = 1.0$ mg/mL), which explains the evolution of the micelle dimensions depicted in Figure 5.

Conclusion

This work intended to answer the question of the topological constraints on the micelle formation in cyclic block copolymers as compared to simple linear diblock copolymers PS−PI system, in selective solvents for the PI block. This was achieved using DLS and direct imaging technique AFM. Micelles made from linear A−B diblock copolymer do not present any constraint (no loops in the core or in the shell), and micelles made from A−B−A triblock copolymer do present one constraint (loops in the core or the shell). Our system, cyclic diblock PS−PI copolymer, combines two constraints, a "loop" in the core and a "loop" in the shell, thus investigating the effect of a "double constraint" on micelle formation. It is established that the morphology of the micelles made from linear block copolymers can be controlled by the temperature, copolymer composition and concentration, method of sample preparation and the solvent quality. In this work, we have shown that the micellar morphology can also be changed by the cyclization of a linear diblock copolymer. The cyclic PS−PI micelles have a very different morphology as compared to micelles made from the analogous linear PS−PI copolymer. On the basis of the present results we can summarize some evidences as follows. (a) The micellar morphology of the micelles made from a diblock copolymer is drastically changed by the chemical bonding of its extremities in order to form a cyclic diblock copolymer. It is noteworthy that both the linear and the cyclic copolymers have exactly the same molar mass and block composition. (b) The size and the polydispersity of the linear PS−PI micelles do not change with the copolymer concentration whereas both parameters are strongly concentration dependent for the micelles made from cyclic PS−PI. (c) The cyclic PS−PI micelles are spherical or discoidal (sunflower-like micelles) at very

low concentrations and start to form wormlike assemblies as more copolymer chains are added. The same effect on the size can be reached by decreasing the quality of the solvent for the inner block. (d) At low concentrations of cyclic PS−PI copolymer, there is coexistence of sunflower-like and wormlike micelles. (e) The cross-section diameter of the cyclic PS−PI micelles does not change with the copolymer concentration and is smaller than the diameter of the linear PS−PI micelles. (f) While the size of the cyclic PS−PI micelles strongly depends on the number of carbons of a *n*-alkane solvent series, the size of the linear PS−PI micelles is the same in all the investigated solvents. (g) The wormlike micelles are very polydisperse and lengthy. According to the AFM pictures, the wormlike micelles length can be longer than 1 μm.

We propose a hypothesis for the particular morphology of the cyclic PS−PI micelles: the elementary units for the wormlike micelle formation are the "sunflower-like" micelles. These micelles (discoid shape) start to self-assemble to avoid the PS-solvent contact, leading to their stacking, and form giant and flexible cylindrical micelles (>1 μm). Other ongoing experiments highlighting the substantial differences between linear and cyclic block copolymers properties are under investigation, particularly at different volume fractions in disordered (solutions), ordered (films) and micellar phase. Those results will be published in forthcoming papers.

Acknowledgment. R.B. acknowledges financial support from the CNRS, la Région Aquitaine, and FEDER. E.M. acknowledges the CNRS for financial support as associated researcher. We would like also to thank the cooperation agreement between France and the "Communauté Française de Belgique" (Tournesol-EGIDE) for financial support. Research in Mons is partly supported by the Belgian Federal Government (PAI V/S: "Chimie Supramoléculaire et Catalyze Supramoléculaire"). R.L. is Directeur de Recherches du Fonds National de la Recherche Scientifique (FNRS, Belgium).

References and Notes

(1) Mortensen, K. *Colloids Surf. A: Physicochem. Eng. Asp.* **2001**, *183−185*, 277.
(2) Ahn, J. H.; Sohn, B. H.; Zin, W. C.; Noh, S. T. *Macromolecules* **2001**, *34*, 4459.
(3) Halperin, A.; Tirrell, M.; Lodge, T. P. *Adv. Polym. Sci.* **1992**, *100*, 31.
(4) Hamley, I. W.; Pedersen, J. S.; Booth, C.; Nace, V. M. *Langmuir* **2001**, *17*, 6386.
(5) Pedersen, J. S.; Hamley, I. W.; Ryu, C. Y.; Lodge, T. P. *Macromolecules* **2000**, *33*, 542.
(6) Won, Y. Y.; Davis, H. T.; Bates, F. S. *Science* **1999**, *283*, 960.
(7) Jenekhe, S. A.; Chen, X. L. *Science* **1999**, *283*, 372.
(8) Park, M.; Harrison, C.; Chaikin, P. M.; Register, R. A.; Adamson, D. H. *Science* **1997**, *276*, 1401.
(9) Torchilin, V. P. *J. Controlled Release* **2001**, *73*, 137−172.
(10) Yang, L.; Alexandridis, P. *Curr. Opin. Colloid Interface Sci.* **2000**, *5*, 132.
(11) Sapurina, I.; Stejskal, J.; Tuzar, Z. *Colloids Surf. A: Physicochem. Eng. Asp.* **2001**, *180*, 193.
(12) Yu, Y.; Zhang, L.; Eisenberg, A. *Macromolecules* **1998**, *31*, 1144.
(13) Zhang, L.; Eisenberg, A. *J. Am. Chem. Soc.* **1996**, *118*, 3168.
(14) Bahadur, P.; Sastry, N. V.; Marti, S.; Riess, G. *Colloids Surf.* **1985**, *16*, 337.
(15) Pacovska, M.; Prochazka, K.; Tuzar, Z.; Munk, P. *Polymer* **1993**, *34*, 4885.
(16) Benmouna, M.; Borsali, R.; Benoît, H. *J. Phys. II (Paris)* **1993**, *3*, 1401.
(17) Borsali, R.; Benmouna, M. *Europhys. Lett.* **1993**, *23*, 263.
(18) Borsali, R.; Benmouna, M.; Benoît, H. *Physica A* **1993**, *201*, 129.
(19) Benmouna, M.; Borsali, R. *J. Polym. Sci. Phys. Ed., Part B* **1994**, *32*, 981.
(20) Borsali, R.; Benmouna, M. *Makromol. Chem. Symp.* **1994**, *79*, 153.
(21) Borsali, R.; Lecommandoux, S.; Pecora, R.; Benoît, H. *Macromolecules* **2001**, *34*, 4229.
(22) Borsali, R.; Schappacher, M.; de Souza Lima, M.; Deffieux, A. Lindner, P. *Polym. Prepr.* **2002**, *43* (1), 201.
(23) Borsali, R.; Minatti, M.; Putaux, J.-L.; Schappacher, M.; Deffieux, A.; Viville, P.; Lazzaroni, R.; Narayanan, T. *Langmuir* **2003**, *19*, 6.
(24) Minatti, M.; Borsali, R.; Schappacher, M.; Deffieux, A.; Soldi, V., Narayanan, T.; Putaux, J.-L. *Macromol. Rapid Commun.* **2002**, *23*, 978.
(25) Su, Y.-l.; Wang, J.; Liu, H.-z. *Langmuir* **2002**, *18*, 5370.
(26) Pruitt, J. D.; Husseini, G.; Rapoport, N.; Pitt, W. G. *Macromolecules* **2000**, *33*, 9306.
(27) Svensson, B.; Olsson, U.; Alexandridis, P.; Mortensen, K. *Macromolecules* **1999**, *32*, 6725.
(28) Goldmints, I.; von Gottberg, F. K.; Smith, K. A.; Hatton, T. A. *Langmuir* **1997**, *13*, 3659.
(29) Couderc, S.; Li, Y.; Bloor, D. M.; Holzwarth, J. F.; Wyn-Jones, E. *Langmuir* **2001**, *17*, 4818.
(30) Kim, J. M.; Sakamoto, Y.; Hwang, Y. K.; Kwon, Y.-U.; Terasaki, O.; Park, S.-E.; Stucky, G. D. *J. Phys. Chem. B.* **2002**, *106*, 2552.
(31) Liu, Y.; Chen, S.-H.; Huang, J. S. *Macromolecules* **1998**, *31*, 2236.
(32) Yang, L.; Alexandridis, P. *Langmuir* **2000**, *16*, 4819.
(33) Gerstenberg, M. C.; Pedersen, J. S.; Majewski, J.; Smith, G. S. *Langmuir* **2002**, *18*, 4933.
(34) Alexandridis, P.; Yang, L. *Macromolecules* **2000**, *33*, 5574.
(35) Caragheorgheopol, A.; Pilar, J.; Schlick, S. *Macromolecules* **1997**, *30*, 2923.
(36) Michels, B.; Waton, G.; Zana, R. *Langmuir* **1997,** *13*, 3111.
(37) Vasilescu, M.; Caragheorgheopol, A.; Caldararu, H.; Bandula, R.; Lemmetyinen, H.; Joela, H. *J. Phys. Chem. B.* **1998**, *102*, 7740.
(38) Shappacher, M.; Deffieux, A. *Macromol. Phys. Chem.* **2002**, *203*, 2463.
(39) Zhong, Q.; Inniss, D.; Kjoller, K.; Elings, V. B. *Surf. Sci. Lett.* **1993**, *290*, L688.
(40) Kopp-Marsaudon, S.; Leclère, Ph.; Dubourg, F.; Lazzaroni, R.; Aimé, J. P. *Langmuir* **2000**, *16*, 8432.
(41) Provencher, S. W. *Comput. Phys. Commun.* **1982**, *27*, 213.
(42) Berne, B. J.; Pecora, R. *Dynamic Light Scattering*, 2nd ed.; Dover: 2000.
(43) Brown, W. *Dynamic Light Scattering*; Clarendon Press: Oxford, England, 1983.
(44) Watanabe, H.; Sato, T.; Osaki, K.; Yao, M. L. *Macromolecules* **1996**, *29*, 3890.
(45) To avoid the agglomeration of the single micelles into clusters and get a clearer picture of their morphology, we prepared a sample (Figure 8A) for which the solvent was freeze-dried. The solution was applied onto the substrate and quickly frozen with liquid nitrogen and then dried under vacuum. At low temperatures, the kinetics of the particles inside the solution and the evaporation rate are both slowed, and what we observe is most probably closer to the real morphology of the micelles in solution.

MA020927E